

# Simulating Vector Control Driver using Maximum Torque Strategy on Current Permanent Magnet Assisted Synchronous Reluctance Motor

Arman Keshavarz<sup>1\*</sup>

<sup>1</sup>Department of Electrical Engineering, Kadous Institute of Higher Education, Rasht, Iran

\*Corresponding author email id: Arman\_keshavarz@yahoo.com

Date of publication (dd/mm/yyyy): 03/04/2018

**Abstract** – Permanent Magnet Assisted Synchronous Reluctance Motor is one of the new motors introduced in transportation industry, which have been introduced as a possible tractions motors in hybrid electric vehicle applications. Achieve maximum torque per ampere (MTPA), knowledge of the motor parameters is necessary. Due to the high ambient temperature inside the engine cavity and also saturation effect, variation of the motor parameters such as inductances and permanent magnets flux density is not avoidable. In this paper, motor equations in biaxial system are described, then a method is presented for vector control considering maximum torque per Ampere. Then, this method is implemented on a Reluctance Synchronous Motor Reinforced with Magnet using Simulink. Simulation results show well performance of the designed control system in a wide range of speed.

**Keywords** – Permanent Magnet Assisted Synchronous Reluctance Motor, Maximum Torque Per Ampere, Vector Control, Electromotive Force.

## I. INTRODUCTION

Growing concerns over environmental issues and the need for sustainable energy have urged for major changes to the way the energy demand is covered in the energy systems [1]. Thus, access to electricity with the highest reliability is a pivotal matter especially in the futuristic digital world which smart grids/microgrids are becoming more mature [2]. Considering smart grids/microgrids as the most important topic of these days, electric vehicles and hybrid electric vehicles have become leading trends in the majority of automotive industries as clean alternatives to conventional vehicles; thus, their efficiency, performance, and control are of extreme importance [3]. Along the same line, recently, there has been significant works in the transportation industry on how to use hybrid electric vehicles as energy storage devices to offer a solution for the environmental and energy sustainability issues [4]. Electrical energy is the most widely used energy carrier for many reasons and this has led to an increasing demand for it [5-8]. This demand can be categorized in some important classes such as Control, Power engineering, transportation, Robotics. Control of systems needs to be robust and reliable [9-10].

In [11] presented an adaptive robust control to tracking problem with the known and unknown parameters in the existence of torque disturbances. Taheri Andani introduced a sliding mode control for solving the reference path tracking and stabilizing issues spherical mobile robot, then

by using Lyapunov function proved the stability of the overall system [12]. Also, control can use in voltage source converter. i.e. a linear quadratic gaussian with loop transfer recovery (LQG/LTR) controller is proposed for a rectifier voltage source converter [13].

Electrical energy has also a key role in robotics application [14, 15]. To meet the increasingly electrical demand, different approaches has been proposed, from developing several generation units and integrating renewables into the grid to active participations of the costumer sides in the power flow balancing [16, 17]. Recently, Permanent Magnet Assisted Synchronous Reluctance Motor (PMA-SynRM) has attracted attentions in transportation industry. This is due to good characteristics of interior permanent magnet synchronous motors and that such motors lack any shortcomings. Good characteristic of IPM-SMs is their high efficiency performance, output power, and gain due to magnetic and reluctance torque [18]. Main disadvantages of IPM-SMs are high current of q axis at high speed operations in flux-weakening region [19] and uncontrolled generator operation as a result of which the inverter exits the circuit [5]. The above problems are due to uncontrolled linkage flux generated by magnets. These fluxes can be resolved by employing PMA-SynRM. In PMA-SynRM structure, number and value of magnets and linkage flux of magnets are very low compared to IPM and dominant torque is the reluctance torque [20]. Compared to conventional reluctance synchronous motors, PMA-SynRM has better torque and power factor. Radiation on photovoltaic system is researched in [21, 22] and optimum tilt angle of photovoltaic systems is investigated. It is showed that experimental and theoretical tilt angles are different in that dust effects photovoltaic systems. Also, it is proved that produced energy by experimentally yearly optimum tilt angle is 3% more than theoretical tilt angle.

In addition, it is said that photovoltaic panel's surface temperature increase up to 5.5% in November and 8.5% in August in [23].

Up to now, few studies have been conducted on PMA-SynRM vector control [24]. In this paper, motor equations are described in biaxial system and then a method is presented for vector control of the system using maximum torque per Ampere (MTPA) method. Then, this method is implemented on a Permanent Magnet Assisted Synchronous Reluctance Motor in Simulink. Simulation results show good performance of the designed control system in a wide range of speeds.

## II. INTRODUCTION AND EXTRACTION OF PMA-SYNRM EQUATIONS

In Fig. 1, a 4-pole rotor of the PMA-SynRM with d-q axes is shown. In PMA-SynRM, magnets are located along q-axis (in IPM, magnets are located along d-axis). Thus, voltage and linkage flux equations of the stator are different from linkage flux and voltage equations of IPM which are described as follows:

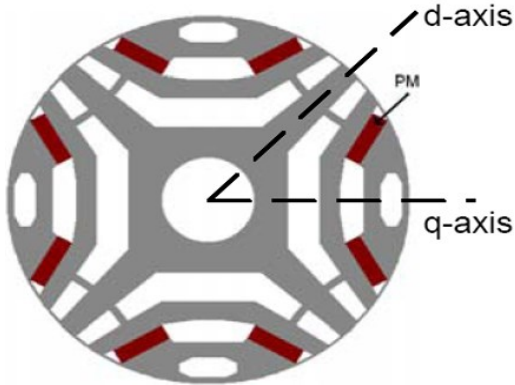


Fig. 1. A 4-pole motor rotor

$$\begin{aligned} v_d &= r_s i_{ds} + \frac{d}{dt} \lambda_{ds} - \omega_r \lambda_{qs} \\ v_q &= r_s i_{qs} + \frac{d}{dt} \lambda_{qs} + \omega_r \lambda_{ds} \end{aligned} \quad (1)$$

$$\begin{aligned} \lambda_{ds} &= L_{ls} i_{ds} + L_{md} i_{ds} = L_{ds} i_{ds} \\ \lambda_{qs} &= L_{ls} i_{qs} + L_{mq} i_{qs} - \lambda_m = L_{qs} i_{qs} - \lambda_m \end{aligned} \quad (2)$$

Steady state equations of d-q axes in PMA-SynRM in the reference system of the rotor are as follows [5]:

$$\begin{aligned} v_{ds}^r - r_s i_{ds}^r - \omega_r \lambda_m &= -L_{qs} \omega_r i_{qs}^r \\ v_{qs}^r - r_s i_{qs}^r &= L_{ds} \omega_r i_{ds}^r \end{aligned} \quad (3)$$

Ignoring leakage inductances, generated electromagnetic torque is obtained as follows:

$$T_e = \frac{3}{2} P ((L_{ds} - L_{qs}) i_{ds} i_{qs} + \lambda_m i_{ds}) \quad (4)$$

Where P shows number of poles. In inverter fed drives it is necessary to have a flexible output voltage [25, 26]. There are two limitations on output voltage and current of inverter-fed drives. Suppose that maximum amplitude of phase voltage and maximum amplitude of line current are  $V_{SM}$  and  $I_{SM}$ , respectively. Thus, operation region is limited using Equations (4) and (5):

$$(i_{ds}^r)^2 + (i_{qs}^r)^2 \leq I_{SM}^2 \quad (5)$$

$$(v_{ds}^r)^2 + (v_{qs}^r)^2 \leq V_{SM}^2 \quad (6)$$

In order to provide load torque, line current amplitude or  $\sqrt{i_{ds}^2 + i_{qs}^2}$  is minimized so that torque is maximized. Using limitations of current in Eq. (5) and assuming that  $L_{ds}$  and  $L_{qs}$  are constant, currents of d and q axes of the stator should satisfy Eq. (7).

$$\frac{dT_e}{dI_s} = 2(L_{ds} - L_{qs}) i_{qs} - \lambda_m + \sqrt{\lambda_m^2 + 4(L_{ds} - L_{qs})^2 i_{ds}^2} = 0 \quad (7)$$

Maximum current amplitude of line  $I_{SM}$  is considered as follows:

$$(i_{ds}^r)^2 + (i_{qs}^r)^2 = I_{SM}^2 \quad (8)$$

From Eq. (7) and (8), maximum accessible torque is obtained as follows:

$$T_e = \frac{3}{2} P ((L_{ds} - L_{qs}) I_{qsM} + \lambda_m) I_{dsM} \quad (9)$$

$$I_{dsM} = \frac{\lambda_m - \sqrt{\lambda_m^2 + 8(L_{ds} - L_{qs})^2 I_{SM}^2}}{4(L_{ds} - L_{qs})} \quad (10)$$

$$I_{qsM} = \sqrt{I_{SM}^2 - I_{dsM}^2} \quad (11)$$

Angular velocity,  $\omega_{rM}$ , can be obtained by substituting (3), (10) and (11) in (6):

$$\begin{aligned} (r_s I_{qsM} + \omega_{rM} L_{ds} I_{dsM})^2 + \\ [r_s I_{dsM} - \omega_{rM} (L_{qs} I_{qsM} - \lambda_m)]^2 &= V_{SM}^2 \end{aligned} \quad (12)$$

Generated electromagnetic torque can be defined based on current angle as in Eq. (13):

$$T_e = \frac{3}{2} P \left( \frac{1}{2} (L_{ds} - L_{qs}) I_s^2 \sin(2\beta) + \lambda_m I_s \cos(\beta) \right) \quad (13)$$

In which,  $I_s$  the amplitude of current and equals to  $I_s = \sqrt{i_{ds}^2 + i_{qs}^2}$ .  $\beta = \tan^{-1}(i_{qs}/i_{ds})$  is Phase Current Angle. To provide MTPA for a given value, it has shown that [22, 23]:

$$\beta = \sin^{-1} \left( \frac{-\lambda_m + \sqrt{\lambda_m^2 + 8(L_{ds} - L_{qs})^2 I_s^2}}{4(L_{ds} - L_{qs}) I_s} \right) \quad (14)$$

To convert from a 3-axis machine to a two-axis, or vice versa, the following relationships are used:

$$f_{dq0s}^r = T \cdot f_{abcs} \quad (15)$$

$$f_{abcs} = T^{-1} \cdot f_{dq0s}^r \quad (16)$$

In which:

$$T(\theta) = \frac{2}{3} \times \begin{bmatrix} \cos(\theta_r) & \cos\left(\theta_r - \frac{2\pi}{3}\right) & \cos\left(\theta_r + \frac{2\pi}{3}\right) \\ \sin(\theta_r) & \sin\left(\theta_r - \frac{2\pi}{3}\right) & \sin\left(\theta_r + \frac{2\pi}{3}\right) \\ \frac{1}{\sqrt{2}} & \frac{1}{\sqrt{2}} & \frac{1}{\sqrt{2}} \end{bmatrix} \quad (17)$$

$$T^{-1}(\theta) = \begin{bmatrix} \cos(\theta_r) & \sin(\theta_r) & \frac{1}{\sqrt{2}} \\ \cos\left(\theta_r - \frac{2\pi}{3}\right) & \sin\left(\theta_r - \frac{2\pi}{3}\right) & \frac{1}{\sqrt{2}} \\ \cos\left(\theta_r + \frac{2\pi}{3}\right) & \sin\left(\theta_r + \frac{2\pi}{3}\right) & \frac{1}{\sqrt{2}} \end{bmatrix} \quad (18)$$

### III. IMPLEMENTATION OF PMA-SYNRM VECTOR CONTROL DRIVE WITH MTPA

In order to implement vector control drive of PMA-SynRM, first the motor should be implemented to ensure its performance. In order to implement the motor, two equations (1) and (2) are considered with the following equation:

$$T_e - T_L = \left(\frac{J}{P}\right) \frac{d}{dt} \omega_r + B\omega_r \quad (19)$$

Motor parameters are given in Table (1):

Table 1. Motor parameters	
$L_{qs} = 8e-3$	$q$ axis inductance
$L_{ds} = 9e-3$	$d$ axis inductance
$r_s = 2.875$	Stator Resistance
$\lambda_m = 0.175$	PM Field (Wb)
$P = 2$	Number of pole pairs
$J = 0.8e-3$	Combined inertia of rotor and load
$B = 0$	Combined viscous friction of rotor and load

In Fig. 2, the block diagram of the implemented motor in Matlab software is shown.

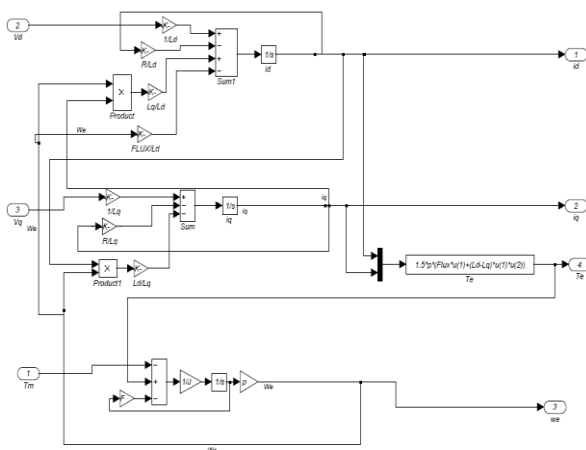


Fig. 2. Block diagram of the implemented motor in Matlab

From (10) and (11), for the implementation of MTPA:

$$I_d = \frac{\lambda_m - \sqrt{\lambda_m^2 + 8(L_{ds} - L_{qs})^2(I_d^2 + I_q^2)}}{4(L_{ds} - L_{qs})}$$

$$\Rightarrow (L_{ds} - L_{qs})I_d^2 - \lambda_m I_d - (L_{ds} - L_{qs})I_q^2 = 0 \Rightarrow$$

$$(L_{ds} - L_{qs})I_q^2 = I_d \left( (L_{ds} - L_{qs})I_d - \lambda_m \right)$$

$$\Rightarrow I_q = \sqrt{I_d \left( I_d - \frac{\lambda_m}{L_{ds} - L_{qs}} \right)} \quad (18)$$

Also, fig. 3 shows the simulation of MTPA.

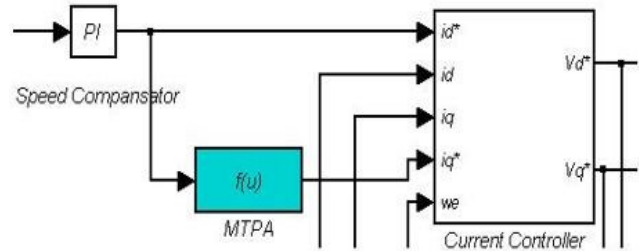


Fig. 3. Implementation of MTPA

### IV. CONTROL UNIT

In order to control the motor, direct current method is used. This method is based on employing two controllers; speed controller and controllers of current on d and q axes. Total diagram of the system is shown in Fig. 4.

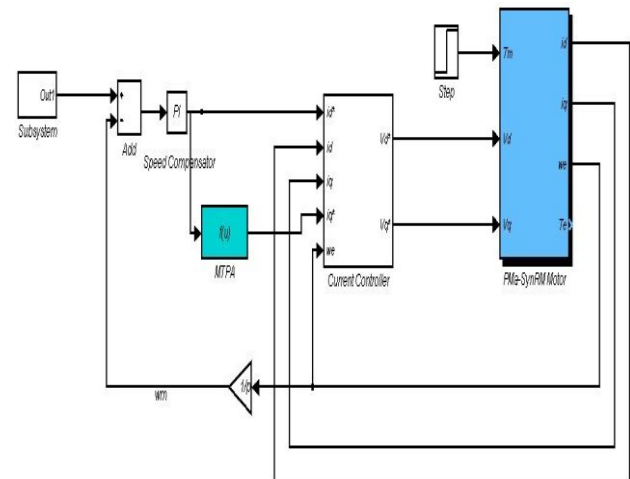


Fig. 4. Total diagram of the system

A PI controller is used to compensate speed error. Output of the speed compensator generated  $i_d^*$  command. That is, speed drop is made possible through applying higher torque with higher  $i_d^*$ . In the next stage, current controller is located. Voltage-current equations of the motor are nonlinear. Product of  $i_{ds}$ ,  $i_{qs}$  and  $\omega_r$  in equations (1) and (2) show this issue. There is a point which reduces this complexity; dynamic of motor currents are faster than its speed dynamic [28-36]. Thus, in design of the current controller, speed can be considered constant in equations (1) and (2). In the next step, an isolation value should be designed for  $i_{ds}$ ,  $i_{qs}$ . This circuit is constructed such that current can be controlled using two linear controllers [37-45]. Due to presence of nonlinear terms  $V_{d0}$  and  $V_{q0}$ , a semi-linear control is implemented. Internal diagram of the current controller block is shown in Fig. 5. Estimating parameters of the controllers is performed using the method given in [24].

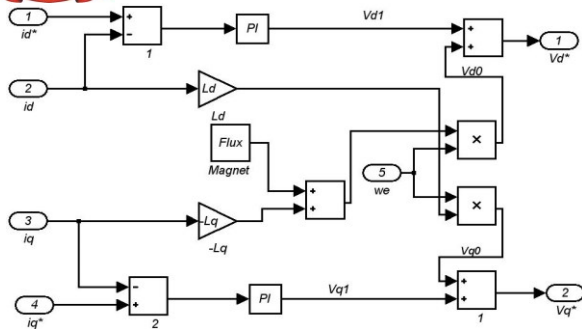


Fig. 5. Internal diagram of the current controller block

As mentioned, parameters of the controllers are estimated using the method given in [21]. This method is comprised of a first order linear system which build motor windings of this system. Compensator and this system comprise a loop. Diagram of this loop is shown in Fig. 6.

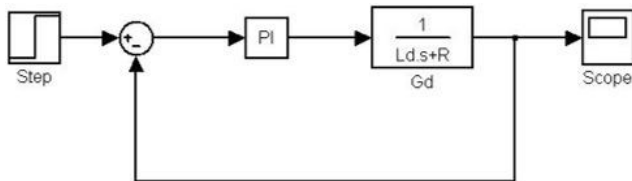


Fig. 6. Estimation of flow controller parameters

Step response of this system is studied. Open loop transfer function has two poles and one zero.

By adjusting ratio of  $\frac{K_I}{K_P}$ , location of zero of the controller is determined. This ratio is selected as 480. Then, speed of the system reaches an acceptable value recommended in [24, 25] by selecting a proper gain for the compensator. Finally,  $K_I = 100000$  and  $K_P = 210$  are selected. In the next step, the current compensator is located in the main system. Speed compensator should be designed. Parameters of this controller are selected through trial and error.

## V. SIMULATION RESULT

Response of the simulated system is shown in Fig. 7.

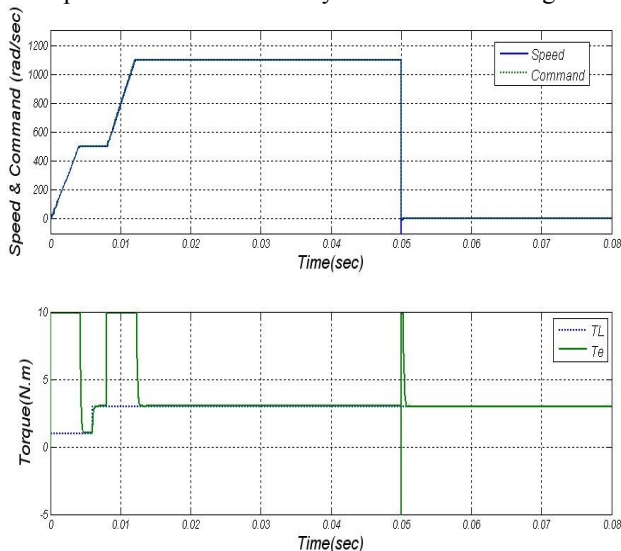


Fig. 7. Internal diagram of the current controller block

For comparison, command waveform is shown in both speed and torque curves. In order to investigate performance above and under nominal speed of the drive, speed command is created as shown. In addition, in order to investigate performance of zero-speed drive, speed command is reduced to zero from a value above nominal speed.

Fig. 7 shows that performance of the drive is very good. Speed and torque track each change in the corresponding command quickly. This result is obtained due to good design and adjustment of the drive control. The designed drive is able to operate above and under nominal speed. In addition, as shown in the simulated waveform, it is also able to operate about zero speed.

Current and voltage waveforms of d and q axes are given in fig. 8 and fig. 9; real voltage and current of the motor are also given in fig. 10 and fig. 11.

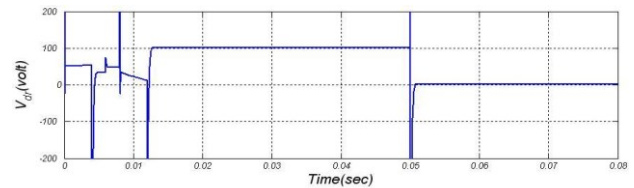


Fig. 8. The axis voltage d and q

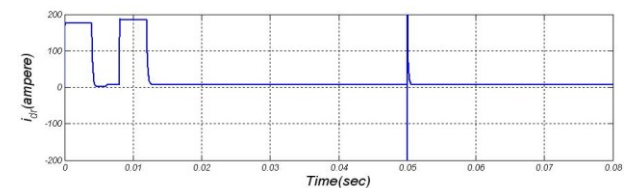


Figure 9: The axis current d and q

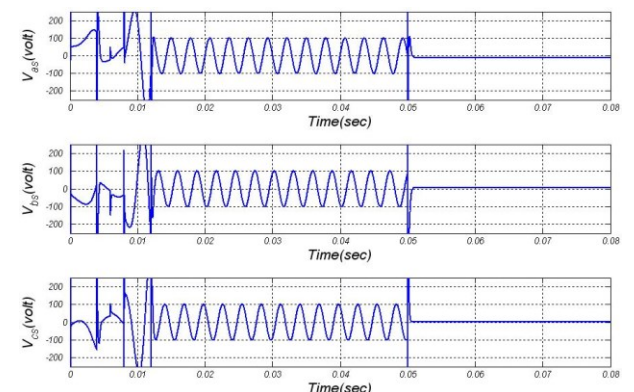


Fig. 10. The shape of the motor voltages

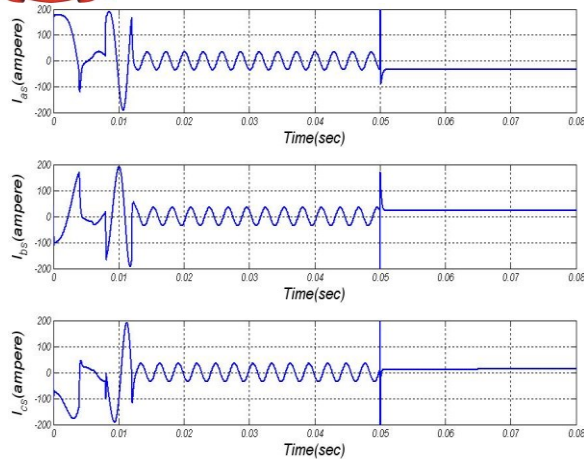


Fig. 11. The shape of the motor currents

## VI. CONCLUSION

In this paper, a method is proposed for vector control of Permanent Magnet Assisted Synchronous Reluctance Motor. First, motor equations in biaxial system are given. Then, MTPA method is described. Then, MTPA method is used for vector control. Suitable current controller parameters are selected. Simulation results indicate well performance of the drive. Speed and torque track each change in the corresponding command quickly. This result is obtained due to well design and adjustment of the drive control system. In addition, the designed drive is able to operate above and under nominal speed and around zero speed. Thus, it is suitable for use in transportation systems.

## REFERENCES

- [1] A. Ghasemkhani; H. Monsef; A. Rahimi-Kian; A. Anvari-Moghaddam, "Optimal Design of a Wide Area Measurement System for Improvement of Power Network Monitoring using a Dynamic Multi objective Shortest Path Algorithm," IEEE Systems Journal, vol. PP, no.99, pp.1-12.
- [2] S. Heydari, S. M. Mohammadi-Hosseininejad, H. Mirsaedi, A. Fereidunian, and H. Lesani, "Simultaneous placement of control and protective devices in the presence of emergency demand response programs in smart grid," *International Transactions on Electrical Energy Systems*, 2018; e2537. <https://doi.org/10.1002/etep.2537>.
- [3] P. Fajri, S. Heydari, and N. Lotfi, "Optimum low speed control of regenerative braking for electric vehicles," in *2017 IEEE 6th International Conference on Renewable Energy Research and Applications (ICRERA)*, San Diego, CA, 2017, pp. 875-879.
- [4] M. Parvizmosaed, A. Anvari-Moghaddam, A. Ghasemkhani, and A. Rahimi-Kian, "Multiobjective dispatch of distributed generations in a grid-connected micro-grid considering demand response actions," 2013.
- [5] Yousefpour, Kamran, Seyyed Javad Hosseini Molla, and Seyyed Mehdi Hosseini, "A Dynamic Approach for Distribution System Planning Using Particle Swarm Optimization," *International Journal of Control Science and Engineering* 5.1 (2015): 10-17.
- [6] Yousefpour, Kamran, "Placement of Dispersed Generation with the Purpose of Losses Reduction and Voltage Profile Improvement in Distribution Networks Using Particle Swarm Optimization Algorithm," *Journal of World's Electrical Engineering and Technology* 2322 (2014): 5114.
- [7] F. Farmani, M. Parvizmosaed, H. Monsef, A. Rahimi-Kian, A conceptual model of a smart energy management system for a residential building equipped with CCHP system, In *International Journal of Electrical Power & Energy Systems*, Volume 95, 2018, Pages 523-536.
- [8] M. Parvizmosaed, F. Farmani, H. Monsef, A. Rahimi-Kian, A multi-stage Smart Energy Management System under multiple uncertainties: A data mining approach, In *Renewable Energy*, Volume 102, Part A, 2017, Pages 178-189.
- [9] Hashemi, S. R., Montazeri, M., & Nasiri, M. (2014). The compensation of actuator delay for hardware-in-the-loop simulation of a jet engine fuel control unit. *Simulation*, 90(6), 745-755.
- [10] Rahmani, B., & Hashemi, S. R. (2015). Internet-based control of FCU hardware-in-the-loop simulators. *Simulation Modelling Practice and Theory*, 56, 69-81.
- [11] Pourseif, T., Andani, M. T., Ramezani, Z., & Pourgholi, M. (2017). Model Reference Adaptive Control for Robot Tracking Problem: Design & Performance Analysis. *International Journal of Control Science and Engineering*, 7(1), 18-23.
- [12] Andani, M. T., & Ramezani, Z. (2017). Robust Control of a Spherical Mobile Robot.
- [13] M. Taheri Andani, H. Pourgharibshahi, Z. Ramezani, and H. Zargarzadeh, "Controller Design for Voltage-Source Converter Using LQG/LTR," in *Power and Energy Conference (TPEC)*, IEEE Texas, 2018, pp. 1-6: IEEE.
- [14] Gharghabi, S. and Safabakhsh, R., 2015, October. Person recognition based on face and body information for domestic service robots. In *Robotics and Mechatronics (ICROM), 2015 3rd RSI International Conference on* (pp. 265-270). IEEE.
- [15] Gharghabi, S., Azari, B., Shamsirdar, F. and Safabakhsh, R., 2016, October. Improving person recognition by weight adaptation of soft biometrics. In *Computer and Knowledge Engineering (ICCKE), 2016 6th International Conference on* (pp. 36-40). IEEE.
- [16] Amini, Mahrz, and Mads Almalkhi. "Trading off robustness and performance in receding horizon control with uncertain energy resources." *Power Systems Computation Conference (PSCC)*, 2018 IEEE. IEEE, 2018.
- [17] Amini, Mahrz, and Mads Almalkhi. "Investigating delays in frequency-dependent load control." *Innovative Smart Grid Technologies-Asia (ISGT-Asia), 2016 IEEE*. IEEE, 2016, pp. 448-453.
- [18] Rahmani, F., Razaghian, F. and Kashaninia, A.R., 2015. Novel Approach to Design of a Class-EJ Power Amplifier Using High Power Technology. *World Academy of Science, Engineering and Technology, International Journal of Electrical, Computer, Energetic, Electronic and Communication Engineering*, 9(6), pp.541-546.
- [19] Ketabdar, M., 2016. Numerical and Empirical Studies on the Hydraulic Conditions of 90 degree converged Bend with Intake. *International Journal of Science and Engineering Applications*, 5(9), pp.441-444.
- [20] Rahmani, F., Razaghian, F. and Kashaninia, A.A., 2014. High Power Two-Stage Class-AB/J Power Amplifier with High Gain and Efficiency. *Journal of Academic and Applied Studies (JAAS)*, 4(6), pp.56-68.
- [21] H. Pourgharibshahi, M. Abdolzadeh, and R. Fadaeinedjad, "Verification of computational optimum tilt angles of a photovoltaic module using an experimental photovoltaic system," *Environmental Progress & Sustainable Energy*, vol. 34, no. 4, pp. 1156-1165, 2015.
- [22] A. Rouholamini, H. Pourgharibshahi, R. Fadaeinedjad, and G. Moschopoulos, "Optimal tilt angle determination of photovoltaic panels and comparing of their mathematical model predictions to experimental data in Kerman," in *Electrical and Computer Engineering (CCECE), 2013 26th Annual IEEE Canadian Conference on*, 2013, pp. 1-4: IEEE.
- [23] A. Rouholamini, H. Pourgharibshahi, R. Fadaeinedjad, and M. Abdolzadeh, "Temperature of a photovoltaic module under the influence of different environmental conditions—experimental investigation," *International Journal of Ambient Energy*, vol. 37, no. 3, pp. 266-272, 2016.
- [24] Ketabdar, M., Moghaddam, A.K., Ahmadian, S.A., Hoseini, P. and Pishdadakhgari, M., 2017. Experimental Survey of Energy Dissipation in Nappe Flow Regime in Stepped Spillway Equipped with Inclined Steps and Sill. *International Journal of Research and Engineering*, 4(5), pp.161-165.
- [25] "Robust Maximum Torque per Amp (MTPA) Control of PM-Assisted SynRM for Traction Applications", P. Niazi, H. A. Toliyat, A. Godarzi, 0-7803-9280-9/05/\$20.00 ©2005 IEEE.

- [26] S. Morimoto, K. Hantanaka, Y. Tong, Y. Takeda, T. Hirasa, "Servo drive system and control characteristics of salient pole permanent magnet synchronous," IEEE Transaction on Industry Application, Volume: 29, pp 338-343, Mar./Apr. 1993.
- [27] S. M. R. Tousei and S. Aznavi, "Performance optimization of a STATCOM based on cascaded multi-level converter topology using multi-objective Genetic Algorithm," in Electrical Engineering (ICEE), 2015 23rd Iranian Conference on, 2015, pp. 1688–1693.
- [28] S. Aznavi, A. Deihimi, "Determining Switching Angles And Dc Voltages In Cascaded Multilevel Inverter for Optimizing Thd in Different Output Voltage Levels using Genetic Algorithm", in 6th International Conference on Technical and Physical Problems of Power Engineering, pp. 449-453, September 2010.
- [29] M. H. Imani, M. Y. Talouki, P. Niknejad and K. Yousefpour, "Running direct load control demand response program in microgrid by considering optimal position of storage unit," 2018 IEEE Texas Power and Energy Conference (TPEC), College Station, TX, USA, 2018, pp. 1-6.
- [30] S. Vaez-zadeh, V.I. John, M. A. Rahman, DSP Control of High Performance Permanent Magnet Synchronous Motor Drives, Part I: Design and Simulation.
- [31] M. H. Imani, K. Yousefpour, M. J. Ghadi and M. T. Andani, "Simultaneous presence of wind farm and V2G in security constrained unit commitment problem considering uncertainty of wind generation," 2018 IEEE Texas Power and Energy Conference (TPEC), College Station, TX, USA, 2018, pp. 1-6.
- [32] Kargarian, Amin, Mahdi Raoofat, and Mohammad Mohammadi. "Probabilistic reactive power procurement in hybrid electricity markets with uncertain loads." *Electric Power Systems Research* 82.1 (2012): 68-80.
- [33] Marvasti, Amin Kargarian, et al. "Optimal operation of active distribution grids: A system of systems framework." *IEEE Transactions on Smart Grid* 5.3 (2014): 1228-1237.
- [34] Amini, M. Hadi, Amin Kargarian, and Orkun Karabasoglu. "ARIMA-based decoupled time series forecasting of electric vehicle charging demand for stochastic power system operation." *Electric Power Systems Research* 140 (2016): 378-390.
- [35] "Rouhani, Mohammadhadi, Mohammad Mohammadi, and Amin Kargarian. "Parzen window density estimator-based probabilistic power flow with correlated uncertainties." *IEEE Transactions on Sustainable Energy* 7.3 (2016): 1170-1181.
- [36] Babaei, Maziar, Thaeer Qunais, and Sherif Abdelwahed. "A linear quadratic tracking based voltage controller for VSI; MVDC shipboard power system application." *Power & Energy Society General Meeting, 2017 IEEE*. IEEE, 2017.
- [37] Bastani, Ali Foroush, Zaniar Ahmadi, and Davood Damircheli. "A radial basis collocation method for pricing American options under regime-switching jump-diffusion models." *Applied Numerical Mathematics* 65 (2013): 79-90.
- [38] Bastani, Ali Foroush, and Davood Damircheli. "An adaptive algorithm for solving stochastic multi-point boundary value problems." *Numerical Algorithms* 74.4 (2017): 1119-1143.
- [39] Tamiz, Mohsen, et al. "AUTMan Humanoid KidSize Team Description Paper."
- [40] Arya, A., Shahmiri, S., Nikkhah, V., & Sarafraz, M. M. (2017). Cooling of High Heat Flux Flat Surface with Nanofluid Assisted Convective Loop: Experimental Assessment. *Archive of Mechanical Engineering*, 64(4), 519-531.
- [41] Arya, A., Sarafraz, M. M., Shahmiri, S., Madani, S. A. H., Nikkhah, V., & Nakhjavani, S. M. (2017). Thermal performance analysis of a flat heat pipe working with carbon nanotube-water nanofluid for cooling of a high heat flux heater. *Heat and Mass Transfer*, 1-13.
- [42] Baferani, Mohammadreza Arab, et al. "A novel arrangement for improving three phase saturated-core fault current limiter (SCFCL)." *Texas Power and Energy Conference (TPEC), 2018 IEEE*. IEEE, 2018.
- [43] Fahimi, Navid, et al. "Investigating the failures of defected silicon rubber insulators in salt-fog chamber." *Texas Power and Energy Conference (TPEC), 2018 IEEE*. IEEE, 2018.
- [44] Rostaghi-Chalaki, Mojtaba, A. Shayegani-Akmal, and H. Mohseni. "HARMONIC ANALYSIS OF LEAKAGE CURRENT OF SILICON RUBBER INSULATORS IN CLEAN-FOG AND

SALT-FOG." *18th International Symposium on High Voltage Engineering*. 2013.

- [45] Rostaghi-Chalaki, Mojtaba, A. Shayegani-Akmal, and H. Mohseni. "A STUDY ON THE RELATION BETWEEN LEAKAGE CURRENT AND SPECIFIC CREEPAGE DISTANCE." *18th International Symposium on High Voltage Engineering (ISH 2013)*. 2013.

## AUTHOR'S PROFILE



**Arman Keshavarz.**

He was born in 1985 in Iran and got his degree at Islamic Azad University of Sari and is a lecturer at Department of Electrical Engineering, Kadous Institute of Higher Education, Rasht, Iran.